ELSEVIER

Journal of Wind Engineering
and Industrial Aerodynamics 95 (2007) 355–369

JOURNAL OF wind engineering AND industrial aerodynamics

www.elsevier.com/locate/jweia

On the use of the k–ε model in commercial CFD software to model the neutral atmospheric boundary layer

D.M. Hargreaves*, N.G. Wright

School of Civil Engineering, University of Nottingham, Nottingham NG7 2RD, UK

Received 14 March 2005; received in revised form 25 July 2006; accepted 10 August 2006
Available online 12 September 2006

Abstract

The k–ε model is routinely used by wind engineers to computationally model the atmospheric boundary layer (ABL). Commercial software is typically used, with the default law of the wall used to model the rough ground surface. By setting appropriate profiles for wind velocity and the turbulence quantities at the inlet, it is often assumed that the boundary layer will be maintained up to the buildings or obstructions in the flow. This paper shows that this is not the case, even in the absence of obstructions, and that the velocity and turbulence profiles decay along the fetch under these default conditions.

By revisiting previous work, it is shown that the neutral ABL can be maintained along a lengthy fetch but only with a modified law of the wall and with a shear stress applied to the top boundary of the domain. For those practitioners who are not able to adopt this more thorough approach, some measures are suggested to mitigate the decay of the boundary layer.

Keywords: CFD; Atmospheric boundary layer; Turbulence

1. Introduction

Computational fluid dynamics (CFD) is now widely used in commercial wind engineering, principally for pedestrian-level wind environment and near-field dispersion

*Corresponding author. Tel.: +44 115 8468079; fax: +44 115 9513898.
E-mail address: David.Hargreaves@nottingham.ac.uk (D.M. Hargreaves).

0167-6105/$ - see front matter © 2006 Elsevier Ltd. All rights reserved.
doi:10.1016/j.jweia.2006.08.002

studies. In this context, use is often made of commercially available CFD codes, because of their ready availability, well-developed interfaces and broad verification and validation. In this modelling, there are two aspects of the real flow situation that are not amenable to direct representation in the CFD and that must, therefore, be modelled in some way. Firstly, the atmospheric boundary-layer (ABL) extends for a considerable distance above the earth's surface relative to the average building height: a CFD model can only represent a smaller, finite distance because of hardware limitations and the complexity of including a meteorological model. Secondly, smaller scale features such as vegetation and small buildings cannot be included in the computational grid and are therefore represented by a roughness model. For the particular class of turbulence model considered in this paper, the k–ε model, the surface roughness is incorporated through a wall function approach that is based on boundary-layer theory for the computational cell immediately adjacent to the wall.

It has been the case for the last decade that the k–ε turbulence model (Launder and Spalding, 1974) and its variants (Yakhot and Orsag, 1986; Speziale, 1987; Tsuchiya et al., 1997) have been the most widely used models in wind engineering and near-field dispersion problems. The majority of the research relating to the k–ε model and its variants (see review by Stathopoulos, 2002) has been concerned with the performance of this and various other turbulence models on flow around cubes and arrays of buildings.

The k–ε model remains in common use despite advances in computer power and the use of other turbulence models such as large eddy simulation (LES), which are increasingly being applied to wind engineering problems. For example, Tseng et al. (2006) used an LES model to look at the dispersion of pollutant in a complex urban environment. They took considerable care in generating the transient inflow conditions from a separate model of an empty fetch. An earlier paper by Nozawa and Tamura (2002), used the LES model to look at a single surface mounted block in a turbulence boundary layer. To generate a boundary layer, velocities at the outlet were recycled to the inlet using periodic boundary conditions over a fetch interspersed with roughness elements. Good agreement was found with experiment in the generation of the boundary layer, which was then applied at the inlet of the model containing the surface mounted block. Allen and Brown (2002) performed LES on a 2D hill in an ABL generated using periodic boundaries in the streamwise direction with an imposed pressure gradient to drive the flow. They found that LES compared favourably with both experimental and k–ε models. As part of an LES simulation of flow past a surface mounted cube, Thomas and Williams (1999) modelled an empty domain to establish an ABL. In the empty domain, good agreement was found between the target logarithmic profile and the computed mean velocity profile at heights above about 0.2 h, where h is the height of the cube.

Much of this modelling, whether using the k–ε or LES models, has been conducted with the buildings embedded in a neutral ABL because buoyancy-induced turbulence need not be modelled. There has, however, always been an underlying problem in that the ABL has often not been modelled in a standard or reproducible manner. These problems have been highlighted in a recent paper by Riddle et al. (2004) in which decay of the velocity profile with distance along the fetch was identified. Walshe (2003), in his PhD thesis, identified the same problem and went on to postulate that the errors were largely due to a spike in the turbulent kinetic energy profile close to the ground.

The most notable and, to date, most successful among those workers who have addressed the modelling of the ABL using CFD are Richards and Hoxey (1993).

They based their approach on a set of assumptions about the ABL. Using these to derive formulae for the velocity and turbulence quantities, they produced a set of boundary conditions to ensure an homogeneous boundary layer. Before describing their approach in more detail, it is worth noting that some aspects of their work have become a standard among practitioners in computational wind engineering. Many users of commercial codes such as Fluent (2003) and CFX (2004) are known to use versions of the Richards and Hoxey inlet boundary conditions for use in CFD simulations. There are many examples of their use, including Blackmore (1996) and Parker and Kinnersley (2004). Other workers have used even more complex expressions for the streamwise component of the wind and turbulence quantities at the inlet. These profiles decayed in the same way as the less complex models due to the inability of the combination of the chosen turbulence model and wall functions to sustain them.

In a recent blind-test of CFD software in modelling wind loading on the full-scale Silsoe cube, as a prerequisite, participants were asked to demonstrate that they could model a sustainable ABL (Richards et al., 2002). It was only Richards among the participants who was able to maintain the turbulent kinetic energy profile along the fetch. The other participants were using largely unmodified versions of two commercial codes, Fluent and CFX. It is worth noting that the majority of computational wind engineering, outside academia, is conducted using commercial software. Many attempts have been made to improve the velocity profiles generated by commercial software. Some recent work by Blocken and Carmeliet (2004) involved the modification of the inlet turbulence kinetic energy profile and surface roughness coefficients to maintain the velocity profile along the fetch. No mention is made, however, of the effect this approach has on the turbulence quantities.

In this paper, the rather contrived situation of a completely empty fetch is used to demonstrate that Richards and Hoxey's inlet boundary conditions by themselves are not sufficient to produce a sustainable ABL when using the k–ε turbulence model. The empty fetch is justifiable on the grounds that most CFD modelling of the ABL has a domain in which there is a sizeable upstream fetch (Franke et al., 2004 suggest five building heights). In such situations, invariably the inlet velocity and turbulence profiles will have changed before the building is reached, which might explain some of the discrepancies between the results from CFD modelling and experimental measurements. It is shown that additional modifications to both the wall boundary condition and the boundary at the top of the domain are required to reproduce the sustainable ABL of Richards and Hoxey. Indeed, the laws of the wall that appear in commercial CFD software require modification before they can be successfully used to sustain an ABL along an empty fetch.

2. The Richards and Hoxey approach

Richards and Hoxey made the following assumptions in attempting to model an homogeneous 2D ABL:

(1) The vertical velocity is zero.
(2) The pressure is constant in both the vertical and streamwise directions.
(3) The shear stress, τ_0 is constant throughout the boundary layer, i.e.

$$\mu_t \frac{\partial u}{\partial z} = \tau_0 = \rho u_\star^2, \tag{1}$$

where μ_t is the turbulent viscosity, u is the streamwise component of the wind speed, ρ is the air density, and $u_\star$ is the friction velocity.

(4) The turbulent kinetic energy, k, and the dissipation rate, ε, satisfy their respective conservation equations, which reduce to,

$$\frac{\partial}{\partial z}\left(\frac{\mu_t}{\sigma_k}\frac{\partial k}{\partial z}\right) + G_k\frac{\varepsilon}{k} - \rho\varepsilon = 0, \tag{2}$$

$$\frac{\partial}{\partial z}\left(\frac{\mu_t}{\sigma_\varepsilon}\frac{\partial \varepsilon}{\partial z}\right) + C_{\varepsilon 1}G_k\frac{\varepsilon}{k} - C_{\varepsilon 2}\rho\frac{\varepsilon^2}{k} = 0, \tag{3}$$

where the production of turbulent kinetic energy is given by

$$G_k = \mu_t\left(\frac{\partial u}{\partial z}\right)^2 \tag{4}$$

and the turbulent viscosity, μ_t, is given by

$$\mu_t = \rho C_\mu \frac{k^2}{\varepsilon}$$

and σ_k, σ_ε, $C_{\varepsilon 1}$, $C_{\varepsilon 2}$ and C_μ are model constants, usually assigned the values 1.0, 1.3, 1.44, 1.92 and 0.09.

Richards and Hoxey then suggest that the above equations can be satisfied by the following:

$$u = \frac{u_\star}{\kappa}\ln\left(\frac{z+z_0}{z_0}\right), \tag{5}$$

$$k = \frac{u_\star^2}{\sqrt{C_\mu}}, \tag{6}$$

$$\varepsilon = \frac{u_\star^3}{\kappa(z+z_0)}, \tag{7}$$

where κ is von Karman's constant and z_0 is the surface roughness length. Eq. (5) is a standard representation of the velocity profile in the ABL. Richards and Hoxey found that Eqs. (5)–(7) satisfy Eq. (2) automatically, but Eq. (3) only when,

$$\sigma_\varepsilon = \frac{\kappa^2}{(C_{\varepsilon 2} - C_{\varepsilon 1})\sqrt{C_\mu}} \tag{8}$$

which gives a value of 1.11 for σ_ε when $\kappa = 0.4$.

3. Numerical model

In order to demonstrate the problems in obtaining a sustainable ABL profile of velocity and turbulence with a standard wall function approach the standard Fluent and CFX codes were used in this investigation, in an attempt to show that the problems are with the modelling of the ABL, rather than a particular piece of software. After demonstrating the deficiencies, suitable amendments to commercial software are proposed, implemented and presented for the ABL. This reflects the situation mentioned earlier, that in this work there

are two types of boundary layer being considered: the standard wall boundary layer and the ABL.

The domain used in the investigation is shown in Fig. 1. The length of the domain was chosen to allow any inlet effects to dissipate and to ensure a developed flow towards the outlet end of the fetch. Note the use of a geometric progression in the vertical grid direction, starting with a grid size of 1 m in the vertical. The lateral width is relatively small as there is no variation in this direction. The grid used is not as fine as possible, but the findings presented here have been seen to hold for various grids. Further, it was decided to use a grid size that is indicative of the grids used for the approach flow in common practice. Were a building to be added, the number of cells would increase due to refinement around the building.

The wind profile used throughout is taken from the blind-test exercise mentioned above (Richards et al., 2002) and is summarised in Table 1. When using a standard law of the wall in commercial CFD, an option is often available for a rough wall—typically specified using a roughness height, ε_R. A common mistake amongst CFD practitioners is to set ε_R equal to z_0, the roughness length. Numerous workers have suggested relationships between ε_R and z_0 (summarised in Franke et al., 2004).

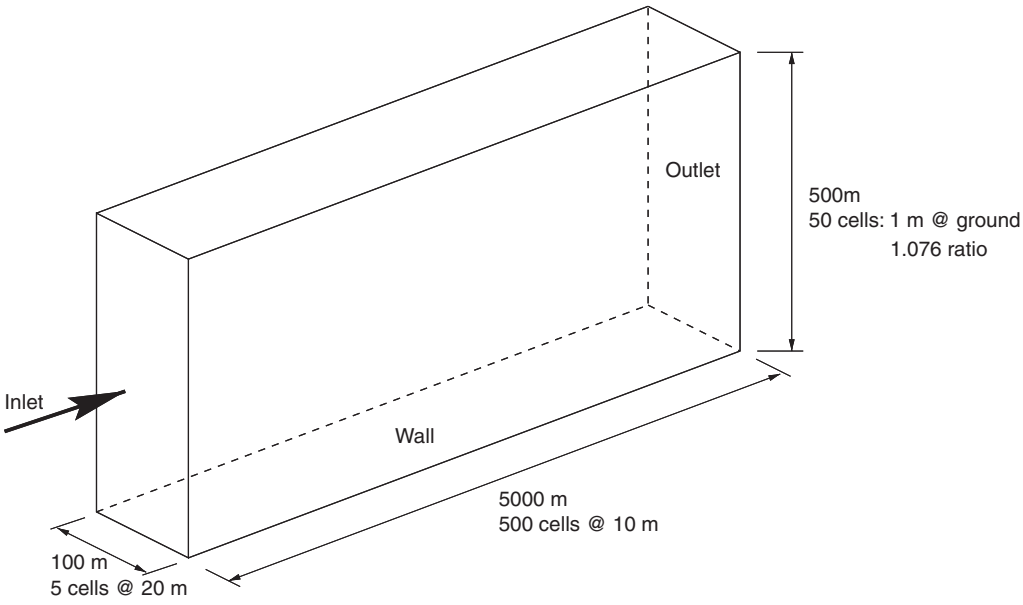

Fig. 1. Schematic of the modelling domain.

Table 1
Wind profile specification

Reference height, z_{ref}	6 m
Roughness length, z_0	0.01 m
Displacement height, h	0 m
Reference mean wind speed, u_{ref}	10 ms^{-1}

The present work uses,

$$\varepsilon_R = 20 z_0 \tag{9}$$

and a more complete justification of this is presented in Section 5.

For Fluent, a series of User-Defined Functions (UDFs) and for CFX, Command Expression Language (CEL) expressions, were used to produce the profiles given by Eqs. (5)–(7) at the upstream inlet. A pressure outlet in Fluent and an outlet boundary in CFX were specified at the downstream end of the fetch. For both codes, symmetry conditions were imposed on the sides and top of the domain. Richards and Hoxey state that a shear stress should be applied at the top of the domain, but since many practitioners ignore this requirement, it was decided that a symmetry condition would suffice for this demonstration. A shear stress condition is implemented later in this work.

For both codes, the standard k–ε model was used with standard wall functions. In both cases, the value of σ_ε was changed from its default value to 1.11. In Fluent, second-order discretisation of the momentum and turbulence transport equations was used; in CFX, the default high resolution scheme was used. These have broadly equivalent accuracy.

Both simulations were run until an acceptable level of convergence was achieved. Grid insensitivity was not tested for because previous experience has shown that the results seen in the next section occur for any reasonable grid used. This statement is backed up by Walshe (2003), who spent considerable time modifying the grid, but to no avail.

No attempt was made to use periodic boundaries at the inlet and outlet and to rely on the surface roughness to create a boundary layer. This approach suffers from the same drawbacks as the approach outlined above in that the boundary layer is not maintained throughout the domain. Further, Apsley (1995) presented an analysis that precludes the use of periodic boundary conditions to model a pressure-driven flow such as the ABL.

4. Results

Fig. 2 is typical of the type of plot produced by computational wind engineers when showing that their simulation of the ABL is satisfactory. It shows profiles of streamwise wind speed, u, turbulent kinetic energy, dissipation rate and $\mathrm{d}u/\mathrm{d}z$ as produced by the Fluent simulation. The profiles are up to a height of $50z_{\mathrm{ref}}$ (300 m) and at distances of 2500 and 4000 m along the domain. The cell-centred values of the variables are plotted for the Fluent simulation: for the results from the CFX simulations, the results are node values. The profiles at 2500 and 4000 m along the fetch are used to demonstrate any variation from a developed boundary layer. In the figures, the key "RH" refers to the inlet profiles of u, k, ε and $\mathrm{d}u/\mathrm{d}z$ given by Eqs. (5)–(7).

At first sight, the profiles of u-velocity are encouraging, with the profile being maintained well. Also, the turbulent dissipation rate is seen to maintain itself along the domain. However, the initially constant value of turbulent kinetic energy is soon lost and does not maintain itself from 2500 through to 4000 m. By zooming into the plots by showing the profiles up to a height of only $5z_{\mathrm{ref}}$ (Fig. 3), the problems near the ground wall boundary become apparent. The spike in the turbulent kinetic energy, seen previously by Walshe (2003), is clear. As Walshe found with CFX, this spike occurs in the second cell above the ground. This, however, is a feature of the k–ε model and in this regard the model deviates from the standard assumptions for the ABL.

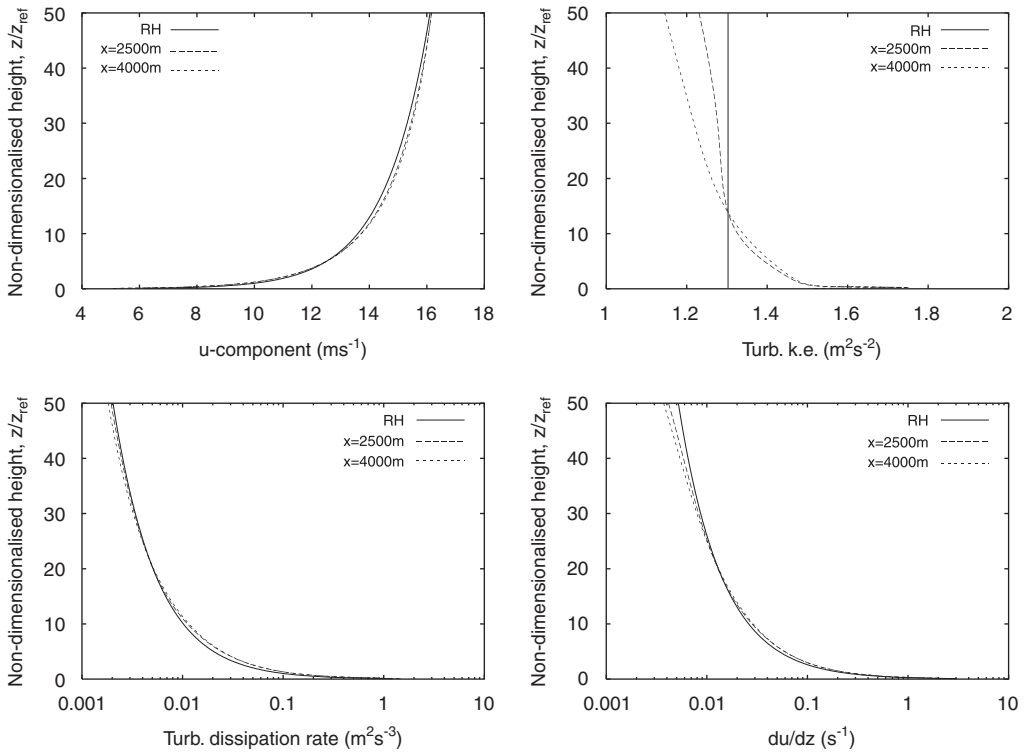

Fig. 2. Plots of u-component of velocity, turbulent kinetic energy, dissipation rate and $\mathrm{d}u/\mathrm{d}z$ for the Fluent simulation, up to a non-dimensionalised height of $50z_{\mathrm{ref}}$.

Far from being a reasonable representation of the ABL, by halfway down the fetch, the velocity in the cell next to the ground has decreased from $6\,\mathrm{ms}^{-1}$ to almost $5\,\mathrm{ms}^{-1}$. The dissipation rate is not maintained along the fetch and the turbulent kinetic energy, as well as exhibiting a large peak, is well above the constant value predicted by Richards and Hoxey.

The results from the CFX simulation display similar trends (Fig. 4). Here profiles only up to a height of $5z_{\mathrm{ref}}$ are shown. The velocity decays along the fetch; the same peak in k is observed, although it is less pronounced; and the dissipation rate decays along the fetch also.

For both Fluent and CFX, the plots of $\mathrm{d}u/\mathrm{d}z$ in the lower reaches of the boundary layer are maintained along the fetch. The production of turbulence kinetic energy in the second and subsequent cells from the wall is essentially proportional to $(\mathrm{d}u/\mathrm{d}z)^2$. The authors believe that the discrepancy in the gradient in the wall-adjacent cell feeds into the production of turbulent kinetic energy in those cells above it, resulting first in the peak and then the move away from the constant value that would be expected.

As an aside, it was noted by Blocken and Carmeliet (2004) that the values of y^+ produced by this approach are in excess of 10,000 for common combinations of z_0 and $u_\star$. The present study found this to be the case also. This is well outside the range of 30 to 300 that is considered necessary for the consistent and accurate application of the logarithmic law of the wall. It is a fact often ignored by computational wind engineers and one that suggests that there may be a need for an alternative definition of y^+ in the modelling of the ABL when rough walls are used.

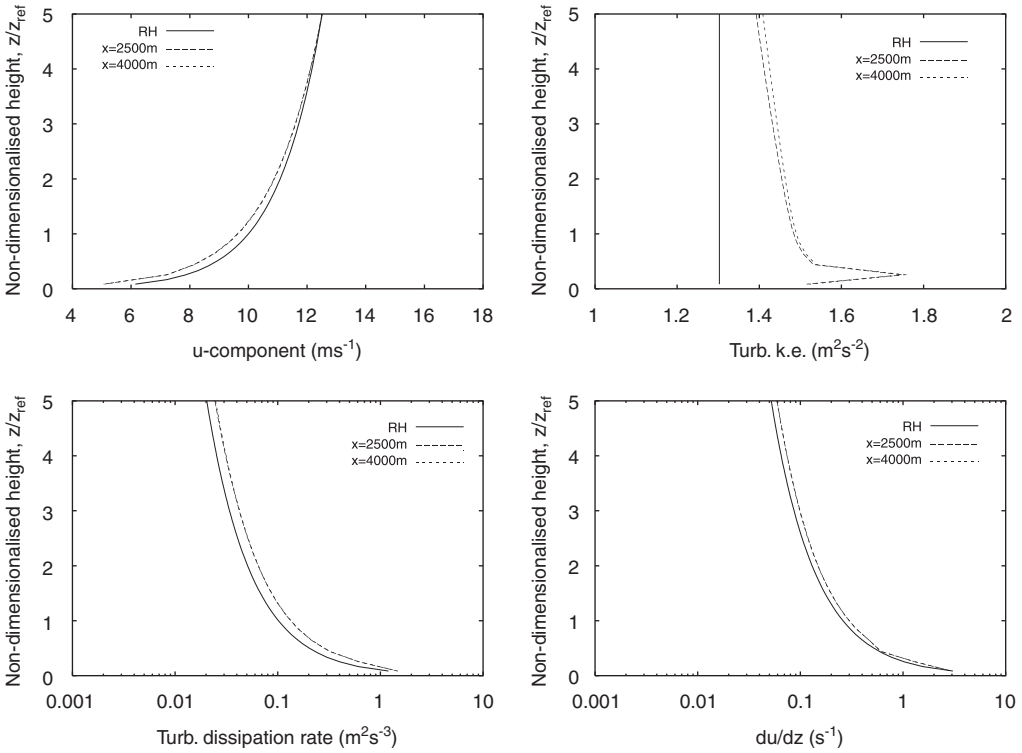

Fig. 3. Plots of u-component of velocity, turbulent kinetic energy, dissipation rate and $\mathrm{d}u/\mathrm{d}z$ for the Fluent simulation, up to a non-dimensionalised height of $5z_{\mathrm{ref}}$.

5. Discussion

Given the above, the question arises as to how Richards and Hoxey were able to maintain the k profile in their approach? The answer lies in the different treatments of the turbulence kinetic energy and dissipation rate in the cell next to the ground between Richards and Hoxey and the commercial software used here. Often taken for granted by computational wind engineers, the specification of the turbulence in the standard law of the wall is key to the success of the model. Richards and Hoxey were using a recompilable version of Phoenics (2005), and therefore had access to the source code. Because of this they were able to modify the wall boundary condition as they wished. A similar ability to modify the wall boundary condition for their own software was demonstrated by Ishihara and Hibi (2002). In the discussion that follows, we will use the initials of Richards and Hoxey (RH) to describe an amalgam of their work.

To show the differences in the wall treatments, it is necessary to take each part of the wall function and compare the implementation in a commercial code (Fluent) and the approach taken by RH (similar conclusions can be drawn by considering CFX). In the series of equations that follows, the standard Fluent form of the equation is presented on the left, the form from RH on the right.

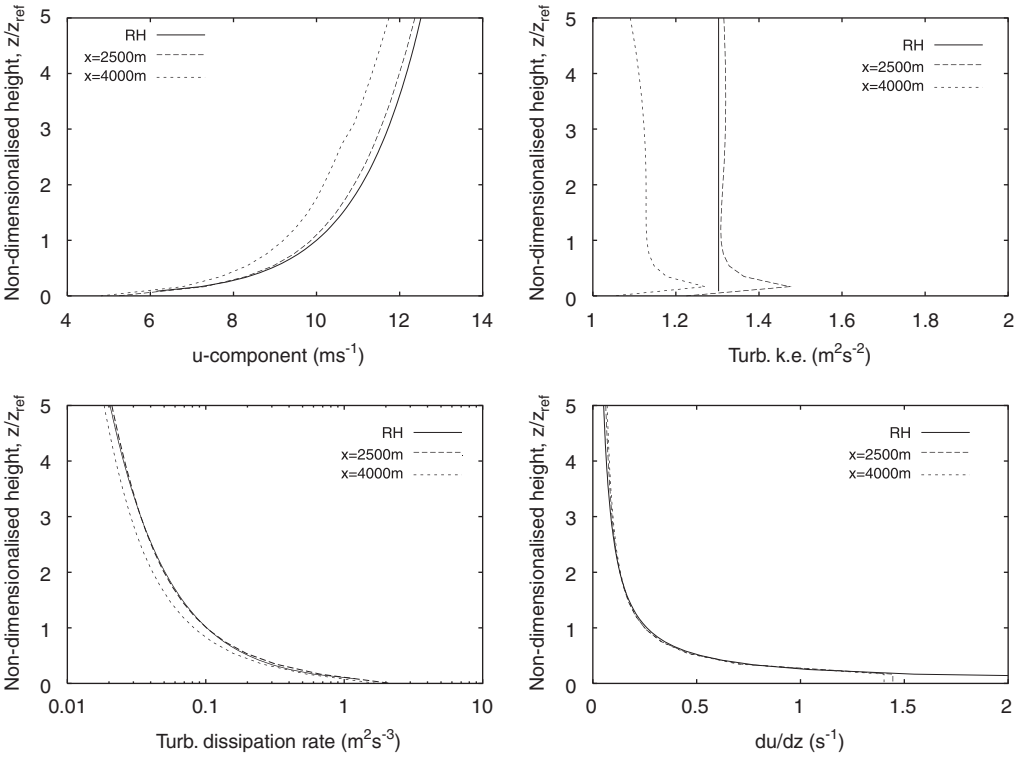

Fig. 4. Plots of u-component of velocity, turbulent kinetic energy, dissipation rate and $\mathrm{d}u/\mathrm{d}z$ for the CFX simulation, up to a non-dimensionalised height of $5z_{\mathrm{ref}}$.

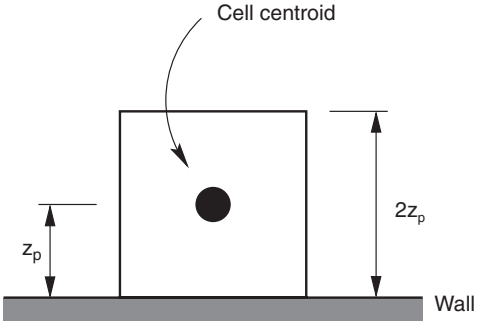

Fig. 5. Schematic of the cell next to the wall.

Consider the shear stress at the wall,

$$\tau_{\mathrm{w}} = \frac{\rho\kappa C_{\mu}^{1/4} k_p^{1/2} u_p}{\ln(Ey^{\star}/(1 + C_s\varepsilon_{\mathrm{R}}^{+}))} \quad \text{versus} \quad \tau_{\mathrm{w}} = \frac{\rho\kappa C_{\mu}^{1/4} k_p^{1/2} u_p}{\ln((z_p + z_0)/z_0)}, \tag{10}$$

where the subscript p refers to the cell adjacent to the wall (see Fig. 5 with z_p being the normal distance from the wall to the cell centre), C_s is the roughness constant,

$\varepsilon_R^+ = \rho u^\star \varepsilon_R/\mu$ and where,

$$y^\star = \frac{\rho C_\mu^{1/4} k_p^{1/2} z_p}{\mu} \quad \text{and} \quad u^\star = C_\mu^{1/4} k_p^{1/2}.$$

In the fully rough regime where $\varepsilon_R^+ \gg 1$, the two shear stress expression are equivalent if $\varepsilon_R = (E/C_s)z_0$. Since C_s defaults to 0.5 in Fluent (and 0.3 in CFX) and E is an empirical constant which takes the value 9.793 in Fluent, this explains the value of 20 seen in Eq. (9). The shear stress is included as a body force in the u-momentum equation and so is fundamental to the correct calculation of the near-wall tangential component of velocity. It can be seen that, by using the rough law of the wall in commercial software, it is possible to reproduce the work of RH.

The standard approach to the modelling of the turbulent kinetic energy in the near-wall cell is to assume a local equilibrium. In other words, the production and dissipation rates of turbulence are approximately equal. In both Fluent and RH, the production rate of turbulent kinetic energy is given by

$$G_k = \tau_w \frac{\partial u}{\partial z}$$

which is often justified from the eddy viscosity hypothesis used in the modelling of the Reynolds stresses. The production rate of turbulent kinetic energy in the wall-adjacent cell is,

$$G_k = \frac{\tau_w^2}{\kappa \rho C_\mu^{1/4} k_p^{1/2} z_p} \quad \text{versus} \quad \bar{G}_k = \frac{\tau_w^2}{\kappa \rho C_\mu^{1/4} k_p^{1/2} 2 z_p} \ln\left(\frac{2z_p + z_0}{z_0}\right) \tag{11}$$

in Fluent (for "standard wall functions") and RH's implementation, respectively. While the default approach in Fluent is to evaluate the production rate at the cell centre, RH evaluate the mean production rate across the cell,

$$\bar{G}_k = \frac{1}{2z_p} \int_0^{2z_p} G_k \, dz = \frac{1}{2z_p} \int_0^{2z_p} \frac{\tau_w^2}{\kappa \rho C_\mu^{1/4} k_p^{1/2} (z + z_0)} \, dz \tag{12}$$

which can be shown to evaluate to the RH production rate in Eq. (11). For the parameter set used in this paper, the relative difference between the Fluent and RH implementations is as follows:

$$\frac{1}{z_p} = \frac{1}{0.5} \quad \text{versus} \quad \frac{1}{2z_p} \ln\left(\frac{2z_p + z_0}{z_0}\right) = \frac{1}{2 \cdot 0.5} \ln\left(\frac{2 \cdot 0.5 + 0.01}{0.01}\right) = 4.62.$$

It should be noted that Fluent also provides "non-equilibrium" wall functions in which the mean cell generation rate is calculated, but here the lower limit of the integration is the boundary of the viscous sub-layer. Use of this non-equilibrium wall function may reduce the above error.

Finally, it is usual in standard wall functions to set the value of the dissipation rate in the cell next to wall, rather than solve for it. The two expressions are,

$$\varepsilon_p = \frac{C_\mu^{3/4} k_p^{3/2}}{\kappa z_p} \quad \text{versus} \quad \varepsilon_p = \frac{C_\mu^{1/2} k u_{\star_g}}{\kappa (z_p + z_0)} \tag{13}$$

which, when $u_{\star_g}$, the ground friction velocity, is equal to $k_p^{1/2}C_\mu^{1/4}$ (the condition for generation being equal to dissipation), the expressions in Eq. (13) are approximately equal—the only difference being z_p and $z_p + z_0$ in the denominator. This difference is due to the shift of origin required by the use of Eq. (5) to ensure $u(z) = 0$ at $z = 0$.

6. Modification of boundary conditions

It would therefore appear to be the differences between the implementation of the standard wall function in the commercial codes and that suggested by RH that is contributing to the problem. To test this further, it was decided to modify Fluent further to include the RH law of the wall. It was realised that the modification of the standard law of the wall in Fluent would be difficult without access to the source code. So, a symmetry boundary condition was used at the ground and the standard k–ε model in Fluent replaced by one written by the authors. To do this, use was made of the User-Defined Scalars (UDSs) in Fluent. One was used to model the turbulent kinetic energy and one for the dissipation rate. By using the standard laminar solver in Fluent and by modifying the viscosity of the air to $\mu_l + \mu_t$, where μ_l is the dynamic viscosity, it was possible to reproduce the standard k–ε model. Within this framework, the shear stress, production rate of turbulent kinetic energy and dissipation rate appropriate to the RH model were applied in the cell next to the ground. In addition, as suggested by RH and often ignored by others, a constant shear stress of $\rho u_\star^2$ was applied at the top boundary.

This model was then used on the same set-up as the unmodified Fluent and CFX software. The results from the RH-modified Fluent model are shown in Fig. 6 up to height of $50z_{\text{ref}}$. RH is again used to denote the RH profiles in Eqs. (5)–(7). It is apparent that the velocity profile is maintained very well, but there is a greater peak in turbulent kinetic energy than that seen previously in the unmodified Fluent model. However, the turbulent kinetic energy soon falls back to the levels predicted by the RH model. Any change in dissipation rate is difficult to discern from this plot and suggests the RH-modified Fluent model is functioning better than the unmodified Fluent one. In the figure, a plot of the turbulent viscosity, μ_t replaces the previously used $\mathrm{d}u/\mathrm{d}z$. This is to show that the turbulent viscosity is well represented except for the upper reaches of the domain, where it deviates slightly from the predicted values. When zooming into the lowest part of the boundary layer (Fig. 7), there is a slight decay in the velocity profile along the fetch, but this is not as large as for the unmodified model. The peak in kinetic energy is again clear and some difference can be seen in the dissipation rate. However, all their quantities are maintained between 2500 and 4000 along the fetch in contrast to the unmodified Fluent model.

It is clear, therefore, that the modifications to the ground law of the wall and the upper shear boundary do produce a sustainable ABL under these typical conditions even if it is not identical to the analytic RH model. The peak in turbulent kinetic energy near the ground may give cause for concern, but it should be noted that it is present to some degree in reality. For instance, from ESDU (1985), the turbulent kinetic energy displays a peak near the ground, as can be seen in Fig. 8. The plot is for the same ABL as used in the rest of this paper. The peak indicates clearly that the RH solution to the Navier–Stokes equations with the k–ε model may require some modification in this respect. The peak seen in the numerical simulations is due to the overprediction of the production term, G_k, in the two or three cells immediately next to the wall.

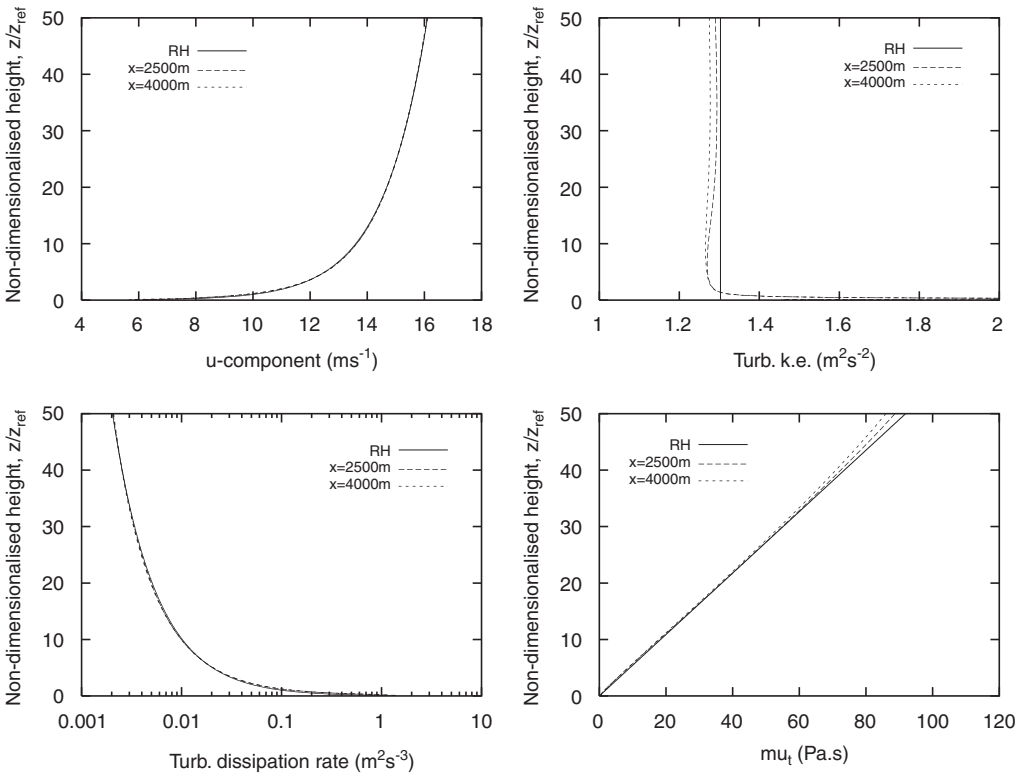

Fig. 6. Plots of u-component of velocity, turbulent kinetic energy, dissipation rate and turbulent viscosity, μ_t, for the RH-modified Fluent simulation, up to a non-dimensionalised height of $50z_{ref}$.

7. Conclusions

It has been shown that, using the default law of the wall and velocity and turbulence profiles specified at the inlet, the ABL will not be sustained along an empty fetch. The reasons for this are:

- The default law of the wall was originally intended for smooth walls or roughness elements the size of sand grains. If an appropriate roughness height is specified, the default law of the wall approximates the approach of Richards and Hoxey.
- The ABL is driven by the geostrophic winds. Simply applying a velocity profile at an inlet and relying on it to be maintained as energy is removed by the shearing at the ground is not appropriate. The flow must be driven by a shear stress at the top boundary. Decay of the inlet velocity profile is due primarily to this shear stress not being applied.
- The over-production of turbulent kinetic energy in the cells nearest the wall, where gradients of velocity are highest, produces a peak in the turbulent kinetic energy.

Richards and Hoxey have gone some way to addressing this problem. By applying *all* of their boundary conditions, it has been shown that the velocity profile of the ABL can be

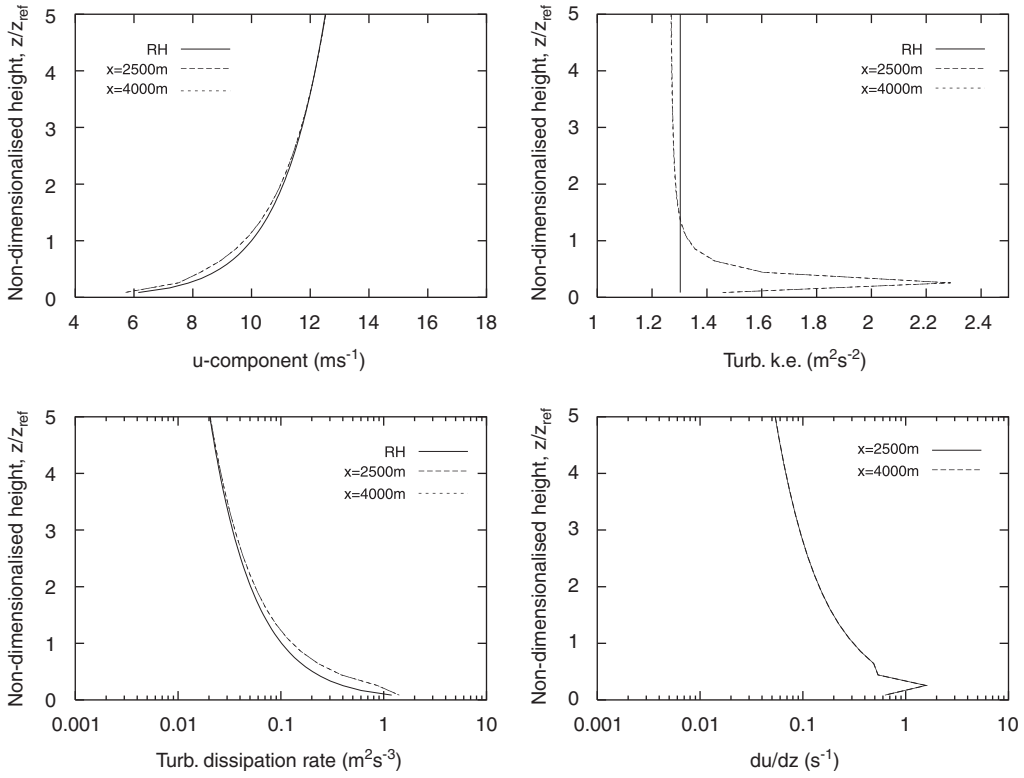

Fig. 7. Plots of u-component of velocity, turbulent kinetic energy, dissipation rate and $\mathrm{d}u/\mathrm{d}z$ for the RH-modified Fluent simulation, up to a non-dimensionalised height of $5z_{\mathrm{ref}}$.

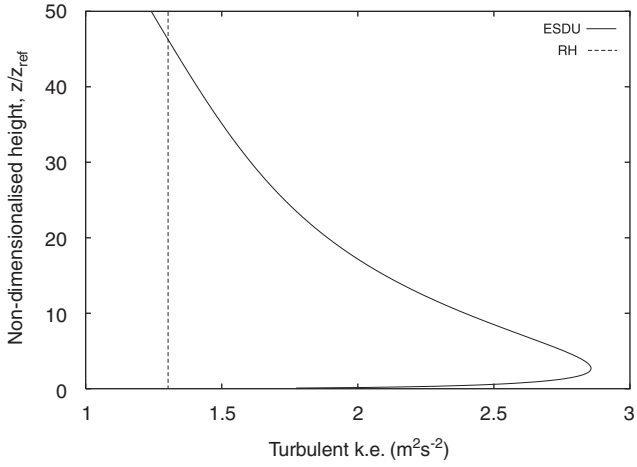

Fig. 8. A plot of the turbulent kinetic energy as predicted by ESDU, 1985.

sustained along the length of the fetch. To do this, however, was not possible without complex modifications to an existing commercial CFD code, Fluent.

The experience of the authors is that many computational wind engineers adopt only a subset of the Richards and Hoxey boundary conditions (i.e. those at the inlet) and assume that the boundary layer will be maintained up to the point at which the building is encountered. Computational wind engineers have seen that fetches are used in wind tunnels and automatically assume one is needed for a CFD study. It is suggested that, if an unmodified commercial code is being used, then as short a fetch as possible is in fact more desirable. This, at the very least, would reduce any changes in the profiles introduced by using a longer fetch. Nevertheless, the fetch should still be long enough that any obstructions, such as buildings, do not affect the inlet flow.

As long as wind engineers continue to routinely use commercial codes such as CFX, Fluent and STAR-CD, the vendors have a duty to revisit the wall boundary condition as it is applied to the ABL. As has been shown, it is not sufficient to rely on a law of the wall originally intended for smooth or sand grain-type roughness walls to model a portion of the much larger ABL. One possible approach would be to provide two types of wall function: one for smooth walls, such as buildings; and one for the ground.

References

Allen, T., Brown, A.R., 2002. Large-eddy simulation of turbulent separated flow over rough hills. Boundary-Layer Meteorol. 102, 177–198.

Apsley, D., 1995. Numerical modelling of neutral and stably-stratified flow and dispersion in complex terrain. Ph.D. Thesis, University of Surrey, 1995.

Blackmore, P.A., 1996. Modelling precipitation deposition rates using CFD methods. Proceedings of the Third U.K. Wind Engineering, Exeter College, Oxford.

Blocken, B., Carmeliet, J., 2004. Modelling atmospheric boundary-layer flow with Fluent: curing the wall-function roughness incompatibility. Proceedings of the Fluent Benelux User Group Meeting, Leuven, Belgium, October 5–6.

CFX 5.7 User's Guide. Ansys Inc., Canonsburg, PA, USA, 2004.

CHAM, Phoenics Software, 2005. CHAM Ltd. Wimbledon, London.

ESDU, 1985. Engineering Sciences Data Item 85020, Engineering Sciences Data Unit, 251-259 Regent Street, London.

Fluent 6.1 User's Guide. Fluent Inc., Lebanon, NH, USA, 2003.

Franke, J., Hirsch, C., Jensen, A.G., Krus, H.W., Schatzmann, M., Westbury, P.S., Miles, S.D., Wisse, J.A., Wright, N.G., 2004. Recommendations on the use of CFD in wind engineering. In: van Beeck, J.P.A.J. (Ed.), Proceedings of the International Conference Urban Wind Engineering and Building Aerodynamics, von Karman Institute.

Ishihara, T., Hibi, K., 2002. Numerical study of turbulent wake flow behind a three-dimensional hill. Wind Struct. 5 (2–4), 317–328.

Launder, B.E., Spalding, D.B., 1974. The numerical computation of turbulent flows. Comput. Methods Appl. Mech. Eng. 3, 269–289.

Nozawa, K., Tamura, T., 2002. Large eddy simulation of the flow around a low-rise building immersed in a rough-wall turbulent boundary layer. J. Wind Eng. Ind. Aerodyn. 90, 1151–1162.

Parker, S.T., Kinnersley, R.P., 2004. A computational and wind tunnel study of particle dry deposition in complex topology. Atmos. Environ. 38, 3867–3878.

Richards, P.J., Hoxey, R., 1993. Appropriate boundary conditions for computational wind engineering models using the k–ε turbulence model. J. Wind Eng. Ind. Aerodyn. 46, 47, 145–153.

Richards, P.J., Quinn, A.D., Parker, S., 2002. A 6 m cube in an atmospheric boundary-layer flow. Part 2. Computational studies. Wind Struct. 5 (2–4), 177–192.

Riddle, A., Carruthers, D., Sharpe, A., McHigh, C., Stocker, J., 2004. Comparisons between Fluent and ADMS for atmospheric dispersion modelling. Atmos. Environ. 38, 1029–1038.

Speziale, C., 1987. On non-linear k–l and k–e models of turbulence. J. Fluid Mech. 178, 459–475.

Stathopoulos, T., 2002. The numerical wind tunnel for industrial aerodynamics: real or virtual for the new millennium? Wind Struct. 5 (2–4), 193.

Thomas, T.G., Williams, J.J.R., 1999. Simulation of skewed turbulent flow past a surface mounted cube. J. Wind Eng. Ind. Aerodyn. 81, 347–360.

Tseng, Y.-H., Meneveau, C., Parlange, M.B., 2006. Modelling flow around bluff bodies and predicting urban dispersion using large eddy simulation. Environ. Sci. Tech. 40, 2653–2662.

Tsuchiya, M., Murakami, S., Mochida, A., Kondo, K., Ishida, Y., 1997. Development of a new k–ε model for flow and pressure fields around bluff body. J. Wind Eng. Ind. Aerodyn. 67, 68, 169–182.

Walshe, J., 2003. CFD modelling of wind flow over complex and rough terrain. Ph.D. Thesis, University of Loughborough.

Yakhot, V., Orsag, S., 1986. Renormalisation group analysis of turbulence; basic theory. J. Sci. Comput. 1, 3–51.